Materials Today Communications 29 (2021) 102796

Contents lists available at ScienceDirect

Materials Today Communications

journal homepage: www.elsevier.com/locate/mtcomm

Enhancing standard finite element codes with POD for reduced order thermal analysis: Application to electron beam melting of pure tungsten

Xielin Zhao [a], Ning An [b], Guangyu Yang [c,*], Jian Wang [c], Huiping Tang [c], Meie Li [d,*], Jinxiong Zhou [a]

[a] State Key Laboratory for Strength and Vibration of Mechanical Structures and School of Aerospace, Xi'an Jiaotong University, Xi'an 710049, People's Republic of China
[b] School of Aeronautics and Astronautics, Sichuan University, Chengdu 610065, People's Republic of China
[c] State Key Laboratory of Porous Metal Materials, Northwest Institute for Nonferrous Metal Research, Xi'an 710016, People's Republic of China
[d] State Key Laboratory for Mechanical Behavior of Materials, School of Materials Science and Engineering, Xi'an Jiaotong University, Xi'an 710049, People's Republic of China

ARTICLE INFO

Dataset link: https://github.com/XJTU-Zhou-group/POD-Abaqus

Keywords:
Proper orthogonal decomposition
Reduced order modeling
Finite element codes
Additive manufacturing
Electron beam melting
Heat transfer

ABSTRACT

This paper describes a numerical scheme that implements reduced order modeling of transient heat transfer problems by enhancing a standard finite element code, ABAQUS, and integrating it with proper orthogonal decomposition (POD). The capability of output and manipulation of matrices, the user subroutine for moving heat source and easy enforcement of boundary conditions, and the powerfulness of pre- and post-processing in the commercial software package are leveraged, resulting in a standard and accessible tool for POD analysis. The proposed strategy is validated through some benchmark heat transfer problems, and it is then applied to simulate the powder-bed electron-beam-melting (EBM) additive manufacturing (AM) process. The pure tungsten with the highest melting point in metals is chosen here as an example, and the first reference on EBM modeling of tungsten is provided, to the best knowledge of the authors. A substantial computation time saving, more than 70%, is achieved for the EBM modeling of single track scanning of a layer of tungsten powder put on a solid substrate. The proposed strategy is readily applicable to other heat transfer problems and AM process simulations, and has practical importance for the users either in industry or academia.

1. Introduction

Heat transfer is a ubiquitous yet crucial phenomenon in modern science and technology, ranging from power plants, energy devices and equipments, engines for various vehicles and transportations, to global climate change, micro-and nano-scale chip cooling, and even biological system such as human body, across various time and length scales. Numerical simulation or thermal analysis plays a crucial role in the design and optimization of heat transfer devices in order to maximize energy utilization and heat transfer efficiency, as a complementary to the expensive and time-consuming experiments.

Among various disciplines where heat transfer is vital, material fabrication and processing belongs to these categories. Classical ways of material processing such as casting, forging, welding and powder metallurgy have brought forward challenging heat transfer problems and have witnessed rapid development of numerical simulation techniques for heat transfer. The recently emerged advanced technology, additive manufacturing (AM), has attracted intensive attentions because it could solve many unsolved problems in classical material processings. AM, on the other hand, also poses even challenging heat transfer problems. Using the widely used AM technique, powder-bed melting, as a representative example, the difficulties arise from modeling powder-bed melting processes, either the selective laser melting(SLM) or the electron-beam melting (EBM), due to the following facts: (1) The powder-bed melting technology uses high energy heat source to melt powders and generate high temperature gradient across regions from the localized melting pool with temperature as high as several thousands degrees celsius to the bulk solidified regions with temperature equal to environmental temperature or the preheating temperature, around several hundreds degrees. This high thermal gradient is coupled to the moving high energy source, and renders the heat transfer problem intrinsically transient and highly nonlinear, and very fined meshing is needed around the melting pool region. (2) Various time and length scales are involved during the thermal analysis of powder-bed melting simulation. [1] The high energy source heat produces instantaneous

* Corresponding authors.
E-mail addresses: yanggy0403@163.com (G. Yang), limeie@xjtu.edu.cn (M. Li).

https://doi.org/10.1016/j.mtcomm.2021.102796
Received 7 July 2021; Received in revised form 11 September 2021; Accepted 11 September 2021
Available online 20 September 2021

and very steep temperature increase at the heat source spot in one or two seconds. But the layer-by-layer AM process would typically take hours or days to complete, and the following cooling process would take even longer period of time. The localized melting pool typically have volume around several 0.1 mm^3, but the real size of a product can have dimensions hundreds or thousands of millimeters. Modeling transient heat transfer across the large variations in time and length scales remains a forbidden task. (3) The powder-bed melting process involves complicated phase transformation and temperature-dependent thermo-physical constant variations. The melted powders transform into liquid phase, and then solidify into solid phase. These phase transformations and the associated latent heat should be tackled carefully. The above-mentioned difficulties involved in the powder-melting AM process render thermal analysis of AM a really time-consuming and computationally expensive process. Our experience of modeling a multi-track EBM process with two layers of powders of pure tungsten each with dimensions 4.2 mm × 4.2 mm × 0.1 mm put on a solid substrate took 19 days of running on a 28-core computer cluster. It is high desirable to develop advanced numerical techniques to speed up the process of thermal analysis, filling the gap between currents AM modeling capability limited to several millimeters and tens of layers and the desperate need for realistic prediction of components with dimensions hundreds of millimeters and fabricated in hundreds or thousands layers.

Conventional methods to solve the transient heat transfer problems consist of discretizing computational domain, approximating the field variables, enforcing initial and boundary conditions, constructing global capacitance (equivalent to mass) matrix and conductance (equivalent to stiffness) matrix, and solving the linear or nonlinear algebraic equations and then stepping forward in time. These routine procedures can be realized by the finite element (FE) method, finite difference method, finite volume methods, and so on. The conventional ways of discretizing and solving the heat transfer problems in the full degrees of freedoms (DOF) are called full order modeling (FOM). The FOM might involves thousands or millions of DOFs, and is extremely cumbersome. To circumvent the difficulties in FOM, efforts have been made to speed up or accelerate the transient heat transfer problems by using the reduced order modeling (ROM). ROM can be categorized into intrusive ROM and non-intrusive ROM depending on whether the method changes the governing equations. See [2,3] for a number of recent advances on ROM including nonlinear intrusive reduction methods, such as discrete empirical interpolation method (DEIM), and various non-intrusive ROM (NIROM) such as machine learning and radial basis function (RBF). Non-intrusive ROM such as machine learning works as a black-box approach without requiring any knowledge of the governing equations of the problem, the core of this method is to construct a cheap-to-evaluate surrogate model with the input/output datasets. Regularly a large number of input/output data is required to train the model sufficiently [4]. On the other hand, intrusive ROM reduces the computational complexity of calculations by reducing the dimensionality of the problem which requires the access to the governing equations and discretized PDE operators. In general, these modifications to governing equations and discretized scheme are not possible when using commercial software. This is true for nonlinear systems because the mass, stiffness matrices and load vector are different and should be updated for each analysis step. For linear systems with constant mass and stiffness matrices and generalized load vector, on the other hand, intrusive ROM is still possible, in the framework of commercial software, by skipping the detailed discretization process and jumping directly to the assembled residual equations. Almost all commercial software provides the functionality of accessing the mass and stiffness matrices, and ROM can be directly performed over the resultant residual equations (which are linear algebraic or differential equations) provided the reducing-order bases are available. We call this weakly intrusive direct ROM and, fortunately, our transient heat transfer problem considered here belongs to this special category. One of the most popular methods for low-order approximation of high dimensional problems is referred to as the proper orthogonal decomposition (POD) technique. Since was first proposed in 1901 by Pearson et al. [5], the POD technique has been developed and provides an efficient approach for ROM analysis in a variety of applications. Han et al. [6] implemented the POD technique on experimentally measured vibration response data to extract the normal mode shapes of a homogeneous and a non-homogeneous free–free beam without measuring the full series of frequency response functions. Białecki et al. [7] developed a POD-based ROM for solving the transient linear heat conduction problems that uses much fewer DOFs than standard numerical techniques with insignificant loss of accuracy. Fic et al. [8] extended the POD-FEM method to solve the nonlinear heat transfer problems and reported a good agreement between solutions obtained by the POD-FEM solver and the standard FEM code. Gaonkar et al. [9] applied multilevel scheme and two level discretization to POD based model order reduction of nonlinear transient heat transfer problems. Zhang et al. [10] adopted POD technique to improve computational efficiency of meshless methods for simulating transient heat conduction problems. In this paper, the POD-based weakly intrusive ROM method is adopted since direct ROM is performed over discretized residual equations. The inherent Galerkin process of transforming PDE to ODE, which is implemented by the commercial software, is utilized directly and thus the Galerkin process in conventional POD-Galerkin methods is avoided.

Constructing snapshot matrix to achieve POD modes and generating and manipulating full DOF system via model reduction sit in the core of POD implementation. Thus far, implementation of POD has mainly been realized by home-made codes developed by different researchers, including FE [7,8], meshless method [11,12], finite difference method [13,14], etc. These in-house computer codes are inaccessible to other researchers and are limited by their capability to handle complicated problems and by the shortcoming of pre- and post-processing functionality. Therefore, it would be desirable to be able to use commercial codes, such as the standard FE code ABAQUS, for advanced ROM analysis. The advantage of implementing ROM in standard codes is obvious: The capacitance and the conductance matrices are automatically computed thus the generation of full DOF matrices is straightforward. The whole arsenal of pre-processing and post-processing of these software makes analysis of the results easier. Finally, the interface as well as the user subroutines provided by these standard codes make analysis of specific problems user-tailored, which is very useful for AM modeling.

This paper describes a method with which standard FE code, ABAQUS, can be utilized to perform POD analysis for accelerated heat transfer problems. The proposed procedure is finally applied to EBM modeling. Here, the EBM of pure tungsten is chosen as an example. This is because tungsten is a refractory metal with the highest melting point as well as the lowest vapor pressure of all metals [15,16]. The manufacturing of tungsten is, however, challenging as it is inherently hard and brittle. Against the limiting factors of established fabrication technologies for tungsten, AM may prove to be an alternative to conventional manufacturing methods due to the more flexibility they can offer. There are a few efforts towards use of AM to fabricate pure tungsten and alloys [17,18]. In spite of these experimental efforts, no effort has been conducted to model the EBM process of tungsten. Although POD-based ROM has been successfully applied in multiple disciplines as described above, the treatment of heat transfer problems during AM process using POD is still untouched so far, to the best of our knowledge, and we actually provide the first reference on POD-based thermal analysis of EBM process of pure tungsten.

This paper is organized as follows. A brief summary of the POD formulation and the enhancement of ABAQUS for transient heat transfer analysis is detailed in Section 2, in particular the output and manipulation of matrices from ABAQUS for thermal analysis. Two benchmark heat transfer problems taken from the literature [19] in

2D and 3D, are studied to validate the proposed method in Section 3. Section 4 presents the modeling of EBM process for pure tungsten. The moving heat source is modeled via a user subroutine in ABAQUS. Finally, some conclusions are given in together with some perspectives for future study in Section 5. We publicize all the data and codes via [https://github.com/XJTU-Zhou-group/POD-Abaqus].

2. Methodology

2.1. Strong and the assembled discretized forms of transient heat transfer problems

The strong form governing equation of a transient heat transfer problem is described by

$$\rho c_p \frac{\partial T}{\partial t} = \nabla \cdot (k \nabla T) + Q(\mathbf{x}, t) \quad in \quad \Omega \tag{1}$$

where ρ is the material density, c_p is the specific heat capacity, T is the temperature, k is the thermal conductivity, Q is the absorbed heat flux which is given by a function of spatial coordinates $\mathbf{x}$ and time t, and Ω is the space–time domain. The governing equation is supplemented by the following initial condition [Eqs. (2)] and boundary conditions [Eqs. (3)–(5)]:

$$T(\mathbf{x}, 0) = T_0 \quad in \quad \Omega \tag{2}$$

$$T = T_W \quad on \quad \Gamma_1 \tag{3}$$

$$-k \nabla T \cdot \mathbf{n} = q_0 \quad on \quad \Gamma_2 \tag{4}$$

$$-k \nabla T \cdot \mathbf{n} = h(T_a - T) \quad on \quad \Gamma_3 \tag{5}$$

where T_0 gives the initial temperature distribution in the domain, T_W denotes the prescribed temperature on Dirichlet boundary Γ_1, and q_0 is the prescribed heat fluxes on Neumann boundary Γ_2, and [Eqs. (5)] dictates the mixed or convection boundary condition with h the convection coefficient and T_a the ambient temperature. The vector $\mathbf{n} = (n_x, n_y, n_z)$ is the unit vector outward normal to the boundary.

A commercial FE software, e.g. ABAQUS, transforms the strong form [Eqs. (1)] into the weak form employing the Galerkin process, discretizes the weak form using FE approximations, and accounts for the boundary conditions [Eqs. (3)–(5)], and finally gives the assembled discretized form of residual equations in the form of :

$$\mathbf{M} \frac{d\mathbf{T}}{dt} + \mathbf{K}\mathbf{T} = \mathbf{F} \tag{6}$$

where $\mathbf{M}$ is the capacitance (mass) matrix, $\mathbf{T}$ is the vector of unknown nodal temperatures, $\mathbf{K}$ is the conductance (stiffness) matrix, and $\mathbf{F}$ is the generalized load vector. The generation of matrices $\mathbf{M}$, $\mathbf{K}$ and vector $\mathbf{F}$ is accomplished by a routine procedure in the context of FE method, and can be realized by programming some in-house codes. The calculation involves shape functions construction and their derivatives evaluations, numerical integration and finite element discretization, etc. The details of this routine procedure can be found in FE textbooks and are omitted here.

Here, recourse is made to standard FE code to get direct access to the stiffness and mass matrices as well as the load vector, an option offered by most commercial packages. In ABAQUS, this option can be easily realized by using keywords and editing the input file. The keyword, ∗MATRIX GENERATE, MASS ∗MATRIX OUTPUT, MASS can export global mass matrix **M**; The keyword, ∗ELEMENT OPERATOR OUTPUT, ASSEMBLE, STIFFNESS, is used to export global stiffness matrix **K**; The keyword, ∗ELEMENT OPERATOR OUTPUT, ASSEMBLE, LOAD, gives load vector **F**. A matlab code was programmed to read and store these matrices exported from ABAQUS.

2.2. Direct ROM using POD modes

After the generation of the mass and stiffness matrices, the next crucial step on POD analysis is the construction of the snapshot matrix and attain the POD modes. In order to collect the snapshots for a given problem, one needs to start with a small number of FOM analysis in ABAQUS. Suppose a series of nodal temperature results for the given heat transfer problem have been obtained by stepping forward in time up to the d step, the snapshot matrix $\mathbf{T}_{snap}$ is assembled as

$$\mathbf{T}_{snap} = [\mathbf{T}_1 \quad \mathbf{T}_2 \cdots \mathbf{T}_i \cdots \mathbf{T}_d] \tag{7}$$

in which $\mathbf{T}_i$ is the response at the ith step and n is the size of T_i which indicates the total number of degrees of freedom. A Python script was coded to read and manipulate the ODB file of ABAQUS to generate the aforementioned snapshot matrix. In general, the time needed to perform the total d steps of FOM analysis would be much shorter than the time believed for the completion of the whole problem.

The singular value decomposition (SVD) is applied to the snapshot matrix, i.e.,

$$\mathbf{T}_{snap} = \mathbf{U}\mathbf{D}\mathbf{V} = \boldsymbol{\Phi}\mathbf{V} \tag{8}$$

where $\boldsymbol{\Phi} = \mathbf{U}\mathbf{D}$ are the POD modes, $\mathbf{D}$ is the singular values matrix and $\mathbf{V}$ is the eigenvector matrix of $\mathbf{T}_{snap}$. The POD modes $\boldsymbol{\Phi}$ can be further approximated by a truncated $\bar{\boldsymbol{\Phi}}$, where $\bar{\boldsymbol{\Phi}}$ only contains the first l modes. On the basis of the selection criterion, the first l order POD basis can be selected accordingly:

$$e(l) = \frac{\sum_{i=1}^{l} \lambda_i}{\sum_{i=1}^{m} \lambda_i} \tag{9}$$

where λ_i is the ith entry of the diagonal matrix $\mathbf{D}$, and $m = min(n, d)$ and $l < m$. The criterion of the minimum l is that $e(l) \geq \delta$ [20], where δ is a truncation value, which is set as 99.999% in this paper. Herein, the relative error $\varepsilon(l)$ of truncated POD bases is defined as $\varepsilon(l) = 1 - e(l)$.

Once the truncated POD modes $\bar{\boldsymbol{\Phi}}$ are obtained, the reduced order forms of matrices and vectors are derived as

$$\bar{\mathbf{M}} = \bar{\boldsymbol{\Phi}}^T \mathbf{M} \bar{\boldsymbol{\Phi}}, \quad \bar{\mathbf{K}} = \bar{\boldsymbol{\Phi}}^T \mathbf{K} \bar{\boldsymbol{\Phi}}, \quad \bar{\mathbf{F}} = \bar{\boldsymbol{\Phi}}^T \mathbf{F} \tag{10}$$

and the full DOF state variables $\mathbf{T}$ is projected onto the POD modes via

$$\mathbf{T} = \bar{\boldsymbol{\Phi}} \bar{\mathbf{T}} \tag{11}$$

This constitutes the sharp contrast of the standard POD-Galerkin to the current POD: in standard POD-Galerkin process, the POD modes are used as test functions and the Galerkin projection is invoked to the original strong form PDE, [Eqs. (1)], and modifications of governing equations and differential operators are needed; the current scheme performs a direct DOF reduction and the projection only involves simple matrix manipulations. The latter is tremendously simpler than the former, but limited to linear systems considered herein.

Therefore, the reduced order ordinary differential equations (ODEs) are given as

$$\bar{\mathbf{M}} \frac{d\bar{\mathbf{T}}}{dt} + \bar{\mathbf{K}} \bar{\mathbf{T}} = \bar{\mathbf{F}} \tag{12}$$

and these reduced order ODEs can finally be solved by explicitly stepping forward in time. When the solution of reduced order system $\bar{T}$ is obtained, the full DOF solution is reconstructed via [Eqs. (11)].

3. Methodology validation

In this section, the aforementioned POD implementation strategy was validated by two benchmark transient heat transfer problems taken from the literature [19], and the analyses results are presented in Figs. 1 and 2.

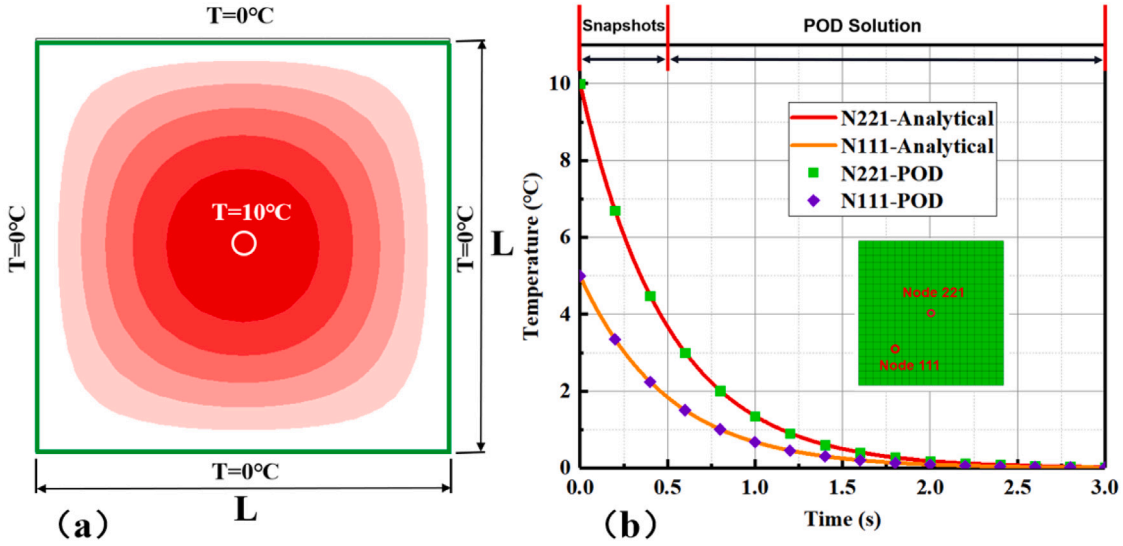

Fig. 1. A 2D heat transfer problem and the validation of the POD method. (a) The schematic of the 2D square problem and its initial and boundary conditions. (b) Validation of the proposed strategy by comparing POD solution with analytical solution. Temperature time histories of two nodes marked on the inserted picture are plotted, and the intervals for snapshot matrix generation as well as the POD solution is discriminated for better view.

Fig. 1(a) schematize a 2D transient heat transfer problem with analytical solution available. The square domain of interest is enforced with prescribed temperatures along four edges and the following nonuniform initial condition:

$$T(x, y, 0) = 10sin(x)sin(y) \tag{13}$$

The initial condition indicates that the centroid of the square has the highest temperature of 10 °C at time 0. The temperature in the domain decays as the distance from the centroid as well as time increase as described by the closed-form solution of this particular problem [19].

$$T(x, y, t) = 10sin(x)sin(y)e^{-2t} \tag{14}$$

Fig. 1(b) plots the analytical solutions in together with the POD solutions for two nodes, 111 and 221, marked in the inserted picture. The physical constants used for the study are: $\rho = 1$ kg/m^3, $C_p = 1$ J/(kg °C), $k = 1$ W/(m °C), and the length of the square L is fixed to be πm. A steady-state is achieved after 3.0 s as shown in Fig. 1(b). FOM was performed over a short period of time from the beginning to 0.5 s, and the full model ABAQUS results were used to generate the snapshot matrix. Thus the interval [0, 0.5 s] is recognized as the snapshot time and POD solutions are calculated from 0.5 s to 3.0 s as marked by the top frame of Fig. 1(b).

Fig. 2(a) shows the schematic picture of a 3D heat transfer problem and its boundary conditions. The 3D domain consists of a hexahedron with a circular hole with diameter $\phi = 0.1$ m. The top and bottom surfaces of the hexahedron is prescribed with convection boundary conditions with convection coefficient h =200 ω /(m^2 °C) with ambient temperature $T_a = 100$ °C. The inner surface of the hole is prescribed with Dirichlet condition with $T_w = 200$ °C. The adiabatic condition is imposed on the four side surfaces of the hexahedron. No analytical solution is available for this 3D problem and the POD solution is plotted against ABAQUS FOM as shown in Fig. 2(b). Temperature histories of three arbitrary nodes, designated by 16, 148, and 504, are plotted. The time period for snapshot matrix generation and the following POD solution are marked for differentiation.

4. EBM modeling of pure tungsten

Having solved the 2D and 3D benchmark problems and validated the accuracy of the proposed POD strategy, we then move on to apply the method to the modeling of EBM process. The pure tungsten was chosen as the candidate material. We firstly solve the transient temperature distribution in a finite solid when heated by a moving double-ellipsoidal heat source on the top surface, which is a typical heat transfer problem in power-bed fusion AM technology as well as in the field of welding. We follow our previous study and enhance ABAQUS by coding a user-subroutine, DLFUX, to model the moving heat source [21–23]. Fig. 3(a) shows the schematic of the problem: A block of bulk material, pure tungsten herein, is heated by an election beam heat source moving at velocity $v = 500$ mm/s. The bottom of the cuboid is enforced with Dirichlet boundary condition, while all other surfaces of the cuboid are assumed to be adiabatic. The reason why this moving source problem was chosen for the study is that an analytical solution is available for this simplified problem [24], which is given as

$$T(x,y,t) = T_p + \frac{3\sqrt{3}Q}{\pi\sqrt{\pi}\rho c} \times \int_0^t 2\frac{exp[\frac{-3(x-vt')^2}{12\alpha(t-t')+c^2}]}{\sqrt{12\alpha(t-t')+c^2}} \cdot \frac{exp[\frac{-3y^2}{\sqrt{12\alpha(t-t')+a^2}} + \frac{-3z^2}{\sqrt{12\alpha(t-t')+b^2}}]}{\sqrt{[12\alpha(t-t')+a^2][\alpha(t-t')+b^2]}} dt' \tag{15}$$

In [Eqs. (15)], $\alpha = k/\rho c_p$ is the thermal diffusion coefficient (k is the thermal conductivity, ρ is the density, c_p is the specific heat capacity); T_p is the preheat temperature; Q is the heat-input; a,b,c are the double ellipsoidal heat source parameters [24,25]. Fig. 3(b) and Fig. 3(c) plot the temperature variations for various points along the scanning trajectory at the same time instant, $t = 0.0042$ s, and for various instants of a fixed point, node 1624, respectively.

We finally come up with the EBM of a single layer of pure tungsten powder put on the top of a solid substrate and scanned by a moving heat source, a typical scenario observed in EBM manufacturing. Fig. 4(a) shows the schematic of the problem. The difference between the problems illustrated in Fig. 3(a) and Fig. 4(a) is noted by the following two facts: A powder layer is present in Fig. 4(a) and it has different material property as the substrate; The top surface of Fig. 4(a) is prescribed by radiation boundary condition, which is more realistic than the adiabatic conditions assumed in Fig. 3(a). Different thermo-physical constants of the powder and the substrate were used for simulation (The parameter of the powder are: $\rho = 10142$ kg/m^3, $C_p = 209$ J/(kg K), $k = 38.6$ W/(m K); The parameter of the substrate are: $\rho = 16904$ kg/m^3, $C_p = 209$ J/(kg K), $k = 97.1$ W/(m K)). The thickness of the powder is 0.05 mm, and the thickness of the substrate is 0.6 mm. A meshing of 24000 eight-node linear heat transfer brick

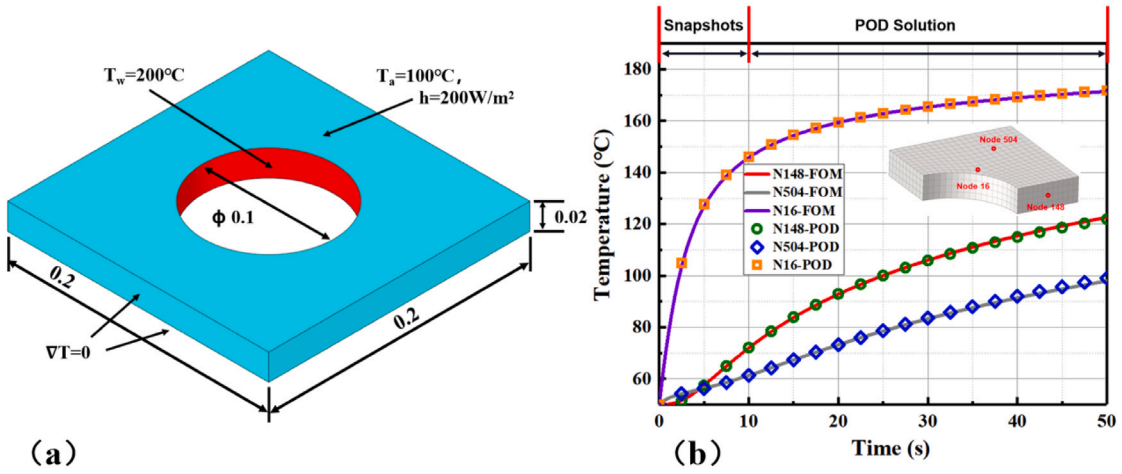

Fig. 2. A 3D transient heat transfer problem and the validation of the proposed method. (a) The schematic of a 3D problem with dimensions and boundary conditions. (b) Comparison of temperature histories of three nodes obtained by ABAQUS FOM and POD ROM, respectively.

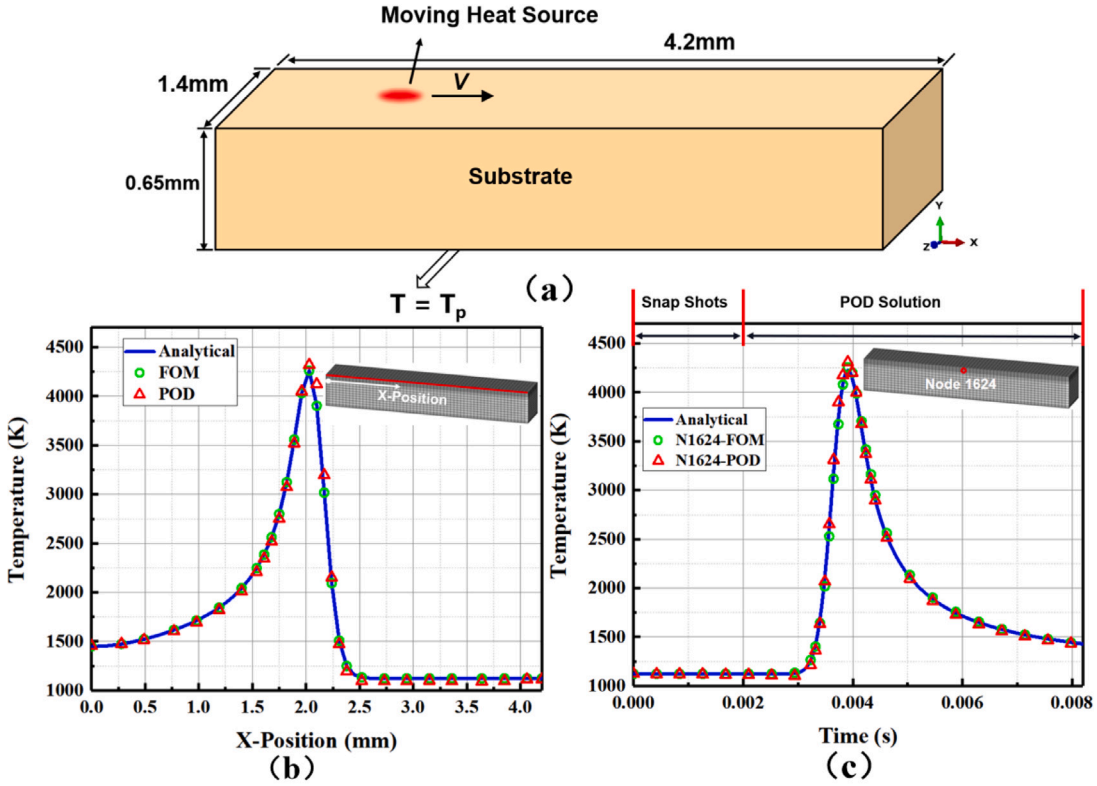

Fig. 3. A typical moving heat source problem with simplified boundary conditions and its POD solution. (a) Dimensions and boundary conditions of a bulk solid heated by a moving source. (b) Analytical and POD solution of the temperature profile for various points along the scanning line at the same time instant $t = 0.0042$ s. (c) Comparison of time histories of temperature given by analytical and POD method for the same node 1642 located on the top surface of the cuboid.

elements (DC3D8), i.e. 26901 nodes, is used in the simulation. The snapshot matrix, $\mathbf{T}_{snap}$, is generated by ABAQUS solutions for a time span of 0.002 s with 200 time steps. The optimal number of truncated POD bases is determined by plotting the relative error $\epsilon(l)$ as a function of the number of POD bases l, as shown in Fig. 5. It can be observed that the relative error function goes down with increasing the number of POD bases, and when the number reaches 30, the relative error of the truncated POD bases is below 0.001%. Hence, 30 POD modes are chosen and then used to predict temperature variation from $t = 0.002$ s to $t = 0.0084$ s.

Fig. 4(b) presents temperature contours obtained from the ABAQUS FOM and that from POD ROM analysis. The reduced order system was solved and stepped forward in time, and the temperature results of the full DOFs were reconstructed by model expansion. The full DOFs solution were then post-processed by using the Tecplot software package. Fig. 4(b) gives temperature contours for three instants, t = 0.001025 s (top), t = 0.0042 s (middle), and t = 0.007175 s (bottom), shown in the top, middle and bottom pictures, respectively. Fig. 4(c) plots the temperature history for a fixed point on the top surface with $x = 2.1$ mm, $y = 0.65$ mm, and $z = 0.7$ mm. Three time instants marked in Fig. 4(b) are inserted in Fig. 4(c). One of the key information that can be extracted from thermal analysis of EBM process is the evolution, morphology and size of the melting poor, which is identified as a crucial factor for EBM process. Fig. 6 presents the comparison between

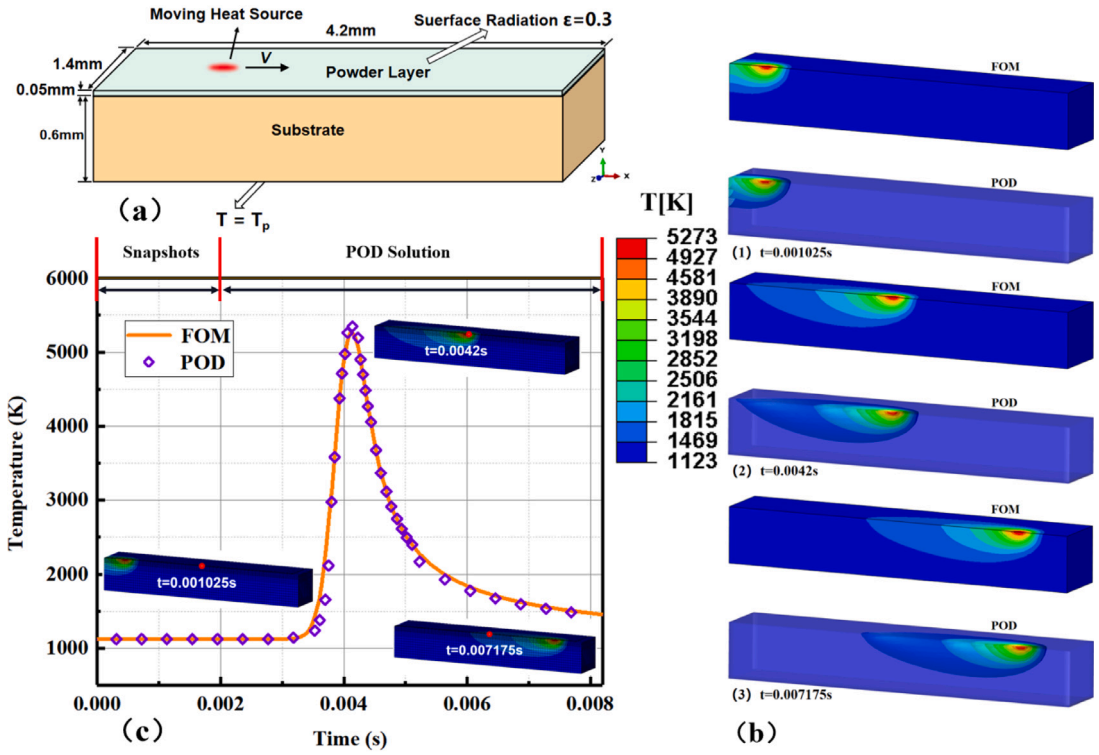

Fig. 4. EBM of a single layer pure tungsten on a solid tungsten substrate. (a) The schematic of the problem. A thin layer of tungsten is heated by the moving source and the top surface is imposed by radiation condition. (b) Comparison between temperature contours obtained by ABAQUS FOM and that by POD ROM analysis for three time instants $t = 0.001025$ s (top), $t = 0.0042$ s (middle), and $t = 0.007175$ s. (c) Temperature time history for a fixed point ($x = 2.1$ mm, $y = 0.65$ mm, $z = 0.7$ mm) on the top surface given by ABAQUS FOM and POD ROM analysis. Three instants in Fig. 4(b) are marked and inserted in (c).

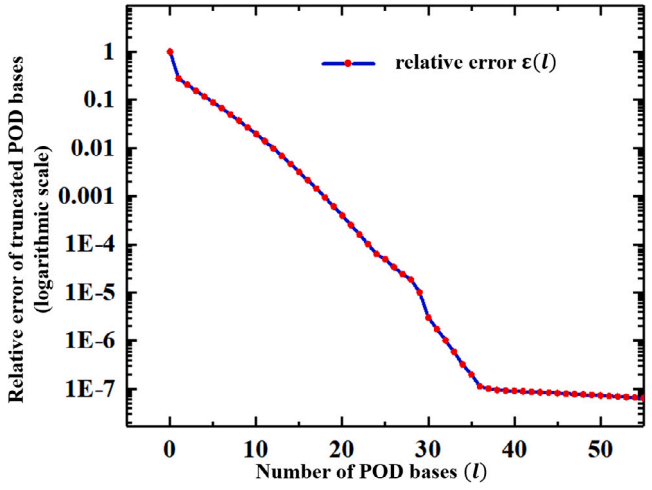

Fig. 5. Relative error of truncated POD bases.

morphology and evolution by ABAQUS FOM analysis and by POD ROM analysis. Good agreement is achieved between the two results. In this study, a workstation with a CPU of Intel Xeon Silver 4114 @ 2.20 GHz and 96G RAM is used. The number of total DOFs of the problem is 26901, and 47 min are needed for ABAQUS FOM analysis on a personal computer, whereas only 1 min is needed for POD analysis in addition to 12 min for snapshot calculation. A substantial computation time saving, 72.3%, is achieved for this particular problem.

5. Conclusion

Modeling transient heat transfer equations is crucial for various areas, and is in general a time-consuming process. It is highly desirable to accelerate heat transfer simulation to speed up the process of product heat design, either from the point view of engineering practice or from the viewpoint of academic research. Reduced order modeling (ROM) is one of the widely used techniques to accelerate heat transfer simulation. Among several choices of ROM analysis, POD is recognized as one of the ROM techniques that is efficient, robust, and powerful, and is used for various dynamic systems. Conventional implementation of POD is realized by coding in-house codes, which prevents its usage due to the inaccessibility of these codes and limited capability of solving complicated engineering problems.

This paper describes a strategy of implementing POD by enhancing the standard finite element code ABAQUS. The full DOF system of transient heat transfer problems is firstly obtained from ABAQUS in together with the construction of the snapshot matrix for model analysis. The matrices of the full DOF system from ABAQUS are then manipulated to yield a reduced system with much smaller number of DOFs. Two benchmark heat transfer problems are solved successfully by the proposed strategy, demonstrating the correctness and feasibility of the method.

We then apply the method and provide the first reference on the EBM process simulation of pure tungsten. An ABAQUS user subroutine was programmed to model the moving heat source. The enhancement of ABAQUS is combined with POD to achieve accelerated modeling of EBM process. A substantial saving of computation time about 70% is achieved for EBM melting of a single layer of tungsten on a solid substrate with 26901 DOFs in total. The numerical scheme presented here is demonstrated via ABAQUS, but the strategy is universal and can be extended to other standard finite element codes, provided the output of matrices is accessible to users. Although the AM process chosen here

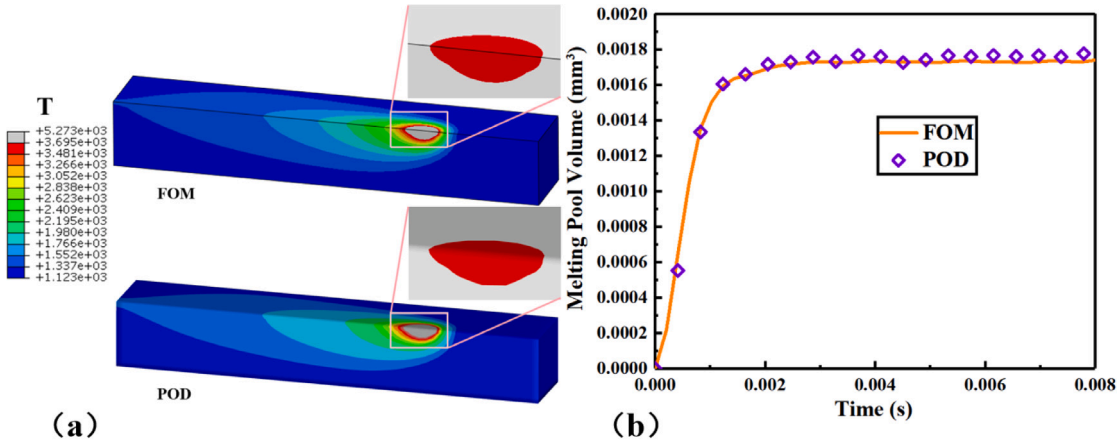

Fig. 6. Comparison of the melting pool predictions given by FOM analysis and by ROM analysis. (a) Morphology of the melting poor. (b) Time history of the volume of melting poor.

is a simplified case of EBM with constant thermo-physical constants and only single track and single layer fabrication has been simulated, the strategy proposed here can be developed and extended further to account for the temperature-dependent properties of materials constant by combining with some non-linear reduction techniques, and more complicated EBM simulations with multiple tracks and multiple layers are underway. The EBM process considered here is in close analogy with the selective laser melting(SLM) process, and the ROM strategy given here can be extended straightforwardly to model other AM processes such as the SLM. We make the codes public, which would facilitate interaction between academia and industry.

Declaration of competing interest

The authors declare that they have no known competing financial interests or personal relationships that could have appeared to influence the work reported in this paper.

Data availability

The raw/processed data required to reproduce these findings are available to download from [https://github.com/XJTU-Zhou-group/POD-Abaqus].

Acknowledgments

This research is supported by a Science Challenge project (TZ2018006) and by National Natural Science Foundation of China (grant 11972277).

References

[1] W. Yan, Y. Qian, W. Ge, S. Lin, W.K. Liu, F. Lin, G.J. Wagner, Meso-scale modeling of multiple-layer fabrication process in selective electron beam melting: inter-layer/track voids formation, Mater. Des. 141 (2018) 210–219.
[2] D. Xiao, F. Fang, A. Buchan, C. Pain, I. Navon, A. Muggeridge, Non-intrusive reduced order modelling of the Navier–Stokes equations, Comput. Methods Appl. Mech. Engrg. 293 (2015) 522–541.
[3] D. Xiao, P. Yang, F. Fang, J. Xiang, C.C. Pain, I.M. Navon, Non-intrusive reduced order modelling of fluid–structure interactions, Comput. Methods Appl. Mech. Engrg. 303 (2016) 35–54.
[4] S. Hijazi, G. Stabile, A. Mola, G. Rozza, Data-driven POD-Galerkin reduced order model for turbulent flows, J. Comput. Phys. 416 (2020) 109513.
[5] K. Pearson, LIII. On lines and planes of closest fit to systems of points in space, Lond. Edinb. Dublin Philos. Mag. J. Sci. 2 (11) (1901) 559–572.
[6] S. Han, B. Feeny, Application of proper orthogonal decomposition to structural vibration analysis, Mech. Syst. Signal Process. 17 (5) (2003) 989–1001.
[7] R. Białecki, A. Kassab, A. Fic, Proper orthogonal decomposition and modal analysis for acceleration of transient FEM thermal analysis, Internat. J. Numer. Methods Engrg. 62 (6) (2005) 774–797.
[8] A. Fic, R.A. Białecki, A.J. Kassab, Solving transient nonlinear heat conduction problems by proper orthogonal decomposition and the finite-element method, Numer. Heat Transfer B 48 (2) (2005) 103–124.
[9] A. Gaonkar, S. Kulkarni, Application of multilevel scheme and two level discretization for POD based model order reduction of nonlinear transient heat transfer problems, Comput. Mech. 55 (1) (2015) 179–191.
[10] X. Zhang, H. Xiang, A fast meshless method based on proper orthogonal decomposition for the transient heat conduction problems, Int. J. Heat Mass Transfer 84 (2015) 729–739.
[11] M. Dehghan, M. Abbaszadeh, Proper orthogonal decomposition variational multiscale element free Galerkin (POD-VMEFG) meshless method for solving incompressible Navier–Stokes equation, Comput. Methods Appl. Mech. Engrg. 311 (2016) 856–888.
[12] M. Dehghan, M. Abbaszadeh, The use of proper orthogonal decomposition (POD) meshless RBF-FD technique to simulate the shallow water equations, J. Comput. Phys. 351 (2017) 478–510.
[13] P. Sun, Z. Luo, Y. Zhou, Some reduced finite difference schemes based on a proper orthogonal decomposition technique for parabolic equations, Appl. Numer. Math. 60 (1–2) (2010) 154–164.
[14] Z.-d. Luo, R.-w. Wang, J. Zhu, Finite difference scheme based on proper orthogonal decomposition for the nonstationary Navier-Stokes equations, Sci. China A 50 (8) (2007) 1186–1196.
[15] E. Lassner, W.-D. Schubert, Properties, Chemistry, Technology of the Element, Alloys, and Chemical Compounds, Vienna University of Technology, Vienna, Austria, Kluwer, 1999, pp. 124–125.
[16] S. Lee, X. Li, Study of the effect of machining parameters on the machining characteristics in electrical discharge machining of tungsten carbide, J. Mater Process. Technol. 115 (3) (2001) 344–358.
[17] A.v. Müller, G. Schlick, R. Neu, C. Anstätt, T. Klimkait, J. Lee, B. Pascher, M. Schmitt, C. Seidel, Additive manufacturing of pure tungsten by means of selective laser beam melting with substrate preheating temperatures up to 1000 °C, Nucl. Mater. Energy 19 (2019) 184–188.
[18] G. Yang, P. Yang, K. Yang, N. Liu, L. Jia, J. Wang, H. Tang, Effect of processing parameters on the density, microstructure and strength of pure tungsten fabricated by selective electron beam melting, Int. J. Refract. Metals Hard Mater. 84 (2019) 105040.
[19] N.N. Minh, N.T. Nha, T.T. Thien, B.Q. Tinh, Efficient numerical analysis of transient heat transfer by consecutive-interpolation and proper orthogonal decomposition, Sci. Technol. Dev. J. 20 (K9) (2017) 5–14.
[20] X. Gao, J. Hu, S. Huang, A proper orthogonal decomposition analysis method for multimedia heat conduction problems, J. Heat Transfer 138 (7) (2016).
[21] N. An, G. Yang, K. Yang, J. Wang, M. Li, J. Zhou, Implementation of abaqus user subroutines and plugin for thermal analysis of powder-bed electron-beam-melting additive manufacturing process, Mater. Today Commun. (2021) 102307.
[22] B. Cheng, S. Price, J. Lydon, K. Cooper, K. Chou, On process temperature in powder-bed electron beam additive manufacturing: model development and validation, J. Manuf. Sci. Eng. 136 (6) (2014).
[23] M. Galati, L. Iuliano, A. Salmi, E. Atzeni, Modelling energy source and powder properties for the development of a thermal FE model of the EBM additive manufacturing process, Addit. Manuf. 14 (2017) 49–59.
[24] N. Nguyen, Y. Mai, S. Simpson, A. Ohta, Analytical approximate solution for double ellipsoidal heat source in finite thick plate, Weld. J. 83 (3) (2004) 82.
[25] V.D. Fachinotti, A.A. Anca, A. Cardona, Analytical solutions of the thermal field induced by moving double-ellipsoidal and double-elliptical heat sources in a semi-infinite body, Int. J. Numer. Methods Biomed. Eng. 27 (4) (2011) 595–607.